Polymer 51 (2010) 2351–2359

Contents lists available at ScienceDirect

Polymer

journal homepage: www.elsevier.com/locate/polymer

Synthesis, characterization and third-order non-linear optical properties of novel fluorene monomers and their cross-conjugated polymers

G. Ramos-Ortíz [a], J.L. Maldonado [a,*], M.C.G. Hernández [b], M.G. Zolotukhin [b,*], S. Fomine [b], N. Fröhlich [c], U. Scherf [c], F. Galbrecht [c], E. Preis [c], M. Salmon [d], J. Cárdenas [d], M.I. Chávez [d]

[a] Centro de Investigaciones en Óptica A.C., A.P. 1-948, 37000 León, Gto., Mexico
[b] Instituto de Investigaciones en Materiales, Universidad Nacional Autónoma de México, Apartado Postal 70-360, CU, Coyoacán 04510, México D.F., Mexico
[c] Macromolecular Chemistry Group, Wuppertal University, Gauss-Str. 20, D-42097 Wuppertal, Germany
[d] Instituto de Química, Universidad Nacional Autónoma de México, Apartado Postal 70-360, CU, Coyoacan 04510, México D.F., México

ARTICLE INFO

Article history:
Received 4 February 2010
Received in revised form
23 March 2010
Accepted 25 March 2010
Available online 31 March 2010

Keywords:
Fluorene polymers
Cubic NLO response
THG Maker-Fringes

ABSTRACT

We designed and synthesized two novel fluorene monomers of **D**–**A**–**D** (donor–acceptor–donor) type (**M1** and **M2**), and their two corresponding polymers (**PM1** and **PM2**) and a copolymer (**CPM**). These high molecular weight, film-forming polymers were obtained from metal-free, superacid-catalyzed reactions of the monomers with *N*-phenylisatin. The cubic NLO response ($\chi^{(3)}$) for these new compounds, in solid thin films, was measured through the use of third-harmonic generation (THG) Maker-Fringes technique at IR wavelengths given values of the order of 10^{-12} esu from which, the corresponding second hyperpolarizabilities (γ) were estimated to be of the order of 10^{-33} esu for monomers and 10^{-31} esu for polymers. Second hyperpolarizabilities have also been estimated theoretically at B3LYP/6-31G(d) level of theory in gas phase and related with the electronic structure of the synthesized molecules.

1. Introduction

There is an enormous interest in developing fluorene derivatives: molecules, oligomers and polymers for different optical applications, such as organic electroluminescence devices (OLEDs) and organic photovoltaic cells (OPVs) [1–10]. Other optical uses are for two photon absorption (TPA) [11–16], and sensors [17]. These fluorene-based compounds are of great interest since they show a strong π–electron conjugation, *i.e.*, large electron delocalization and, additionally, high fluorescent efficiency. Fluorene is a suitable arylene moiety because it is easy to substitute with solubilizing groups at its 9-position [18].

Non-linear optical (NLO) properties have been measured for a few fluorene systems [18,19]. It is believed that the strong π–electron conjugation is crucial factor in attaining high optical non-linearities and so, it is of great interest to identify or understand the structure–property relationship. This knowledge is very important for a rational design of new second and third-order NLO materials based on both low molecular weight molecules and polymers. The electronic transitions of the fluorene-based compounds can be readily tuned by varying the nature of the co-units in the main chain, and the intra-chain charge transfer between the electron-deficient and electron-excessive units can enhance their NLO properties. Additionally, optical phenomena in fluorene containing polymers can be controlled by the introduction of cross-conjugated segments into the main chain. In cross-conjugation three groups are present, two of which are not conjugated with each other, although each is conjugated with the third one [20].

In this work, we have designed and synthesized two novel fluorene monomers of **D**onor–**Ac**ceptor–**D**onor type (**M1** and **M2**) (see chemical structures in Fig. 1), and two corresponding polymers (**PM1** and **PM2**) and a copolymer (**CPM**).

Linear (absorption and fluorescence) and NLO properties of these new fluorene containing monomers and (co)polymers are reported. The third-order optical susceptibility $\chi^{(3)}$ $(-3\omega,\omega,\omega,\omega)$, was estimated through THG Maker-Fringes technique [21].

2. Results and discussion

2.1. Synthesis of monomers and polymers

Monomers **M1** and **M2** have been prepared using organo metal catalyzed aryl–aryl Suzuki cross-coupling (see Experimental

* Corresponding authors.
E-mail addresses: jlmr@cio.mx (J.L. Maldonado), zolotukhin@iim.unam.mx (M.G. Zolotukhin).

0032-3861/$ – see front matter © 2010 Elsevier Ltd. All rights reserved.
doi:10.1016/j.polymer.2010.03.046

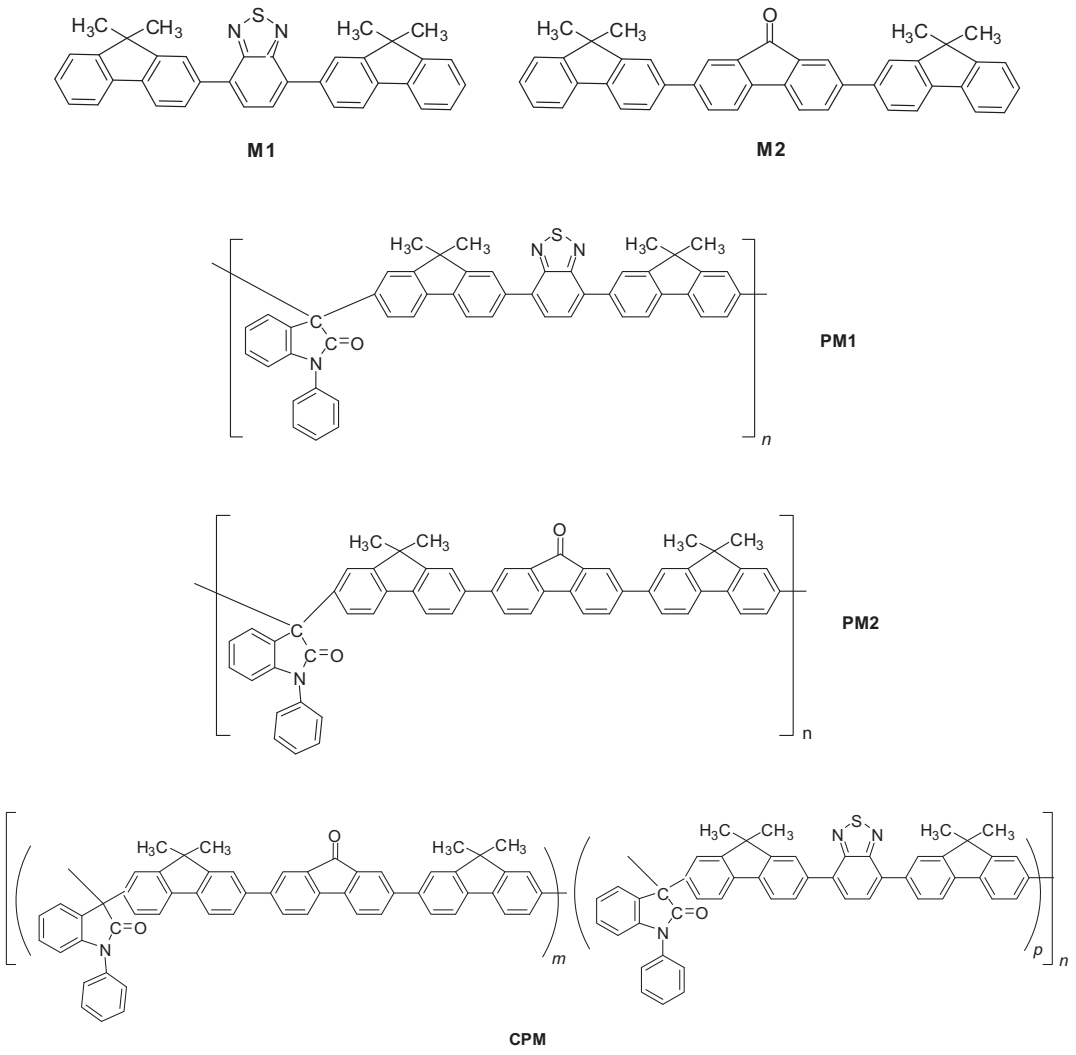

Fig. 1. Chemical structures of the five analyzed fluorene monomers and polymers.

section). The monomers were obtained in good yields; their structural integrity and high purity were confirmed.

Polymers **PM1**, **PM2** and **CPM** were obtained by superacid-catalyzed polyhydroxyalkylation of monomers **M1** and **M2** (and their mixture) with *N*-phenylisatin [22]. Thus, the synthesis of polymer **PM1** proceeds as electrophilic aromatic substitution according to the following Scheme 1.

Since it is often very difficult to achieve high regioselectivity in electrophilic aromatic polycondensation reactions, each polymer was subjected to structural studies by NMR spectroscopy and taking advantage of the good solubility of the polymers obtained in $CDCl_3$. As an example, the ^{13}C NMR spectrum of polymer **PM1** is presented in Fig. 2a.

The spectrum is very well resolved and shows all anticipated resonances, pointing to strictly 2,7-substituion in fluorene fragments. It should be noted that resonances of protons (particularly, in isatin and *N*-phenyl nuclei) are somewhat broadened and do not allow for their correct assignment. Similarly, NMR studies of polymers **PM2** and **CPM** revealed high regioselectivity of polymer-forming reactions leading to linear structures with *para*-substitution in the main chain. The ^{1}H and ^{13}C NMR spectra and the signal assignments of polymer PM2 are given in Fig. 2b. Polymers are soluble in common organic solvents, such as chloroform, methylene chloride, tetrahydrofurane, *N*,*N*-dimethylformamide and *N*-methylpyrrolidon. Transparent, strong, and flexible films could be cast from the polymer solutions.

The obtained polymers possess a high molecular weight and a reasonably narrow polydispersity. According to GPC data, the molecular weights M_w and M_n for **PM1**, **PM2** and **CPM** were found to be: 1.22×10^5 and 8.47×10^4, 8.55×10^4 and 6.07×10^4, 1.55×10^5 and 1.05×10^5 g/mol, respectively. In thermo gravimetric measurements (TGA) the temperature of 2% weight loss in air was found to be ~400 °C. DSC analysis did not reveal any thermal transitions before decomposition of the polymer starts.

2.2. Electronic structure of a polymer chain

Quantum mechanics calculations [23] performed for a model compound depicted in Fig. 3 has shown the presence of electronic coupling between fluorene fragments through a sigma bridge. This effect can be clearly seen in Fig. 4, representing the HOMO energy level of the model compound optimized at HF/3-21G level of theory.

As seen from Fig. 4, the HOMO level has contributions from π-orbitals of both fluorene fragments and sigma orbitals of spiro-tetrahedral carbon, which connects two π-systems. As a matter of fact, this type of connections between different aromatic blocks in the main chain proceeds through homoconjugation mechanism

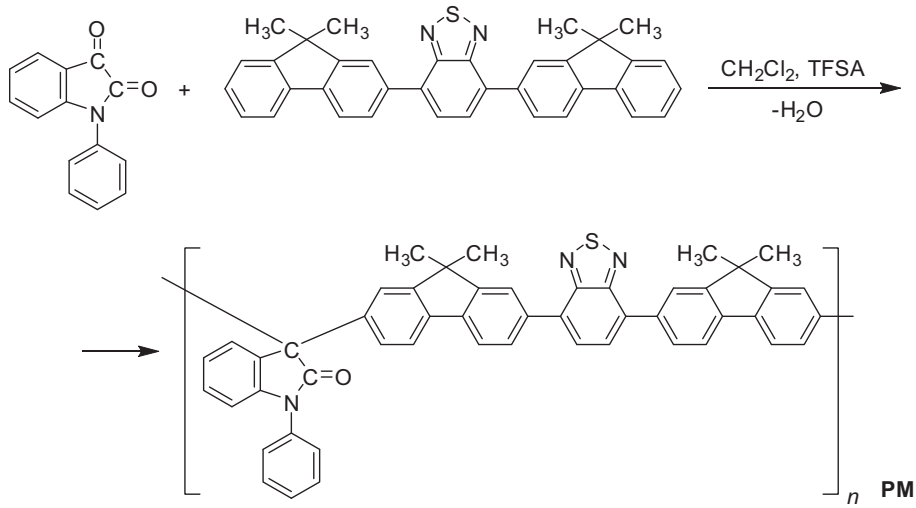

Scheme 1. Synthesis of polymer **PM1**.

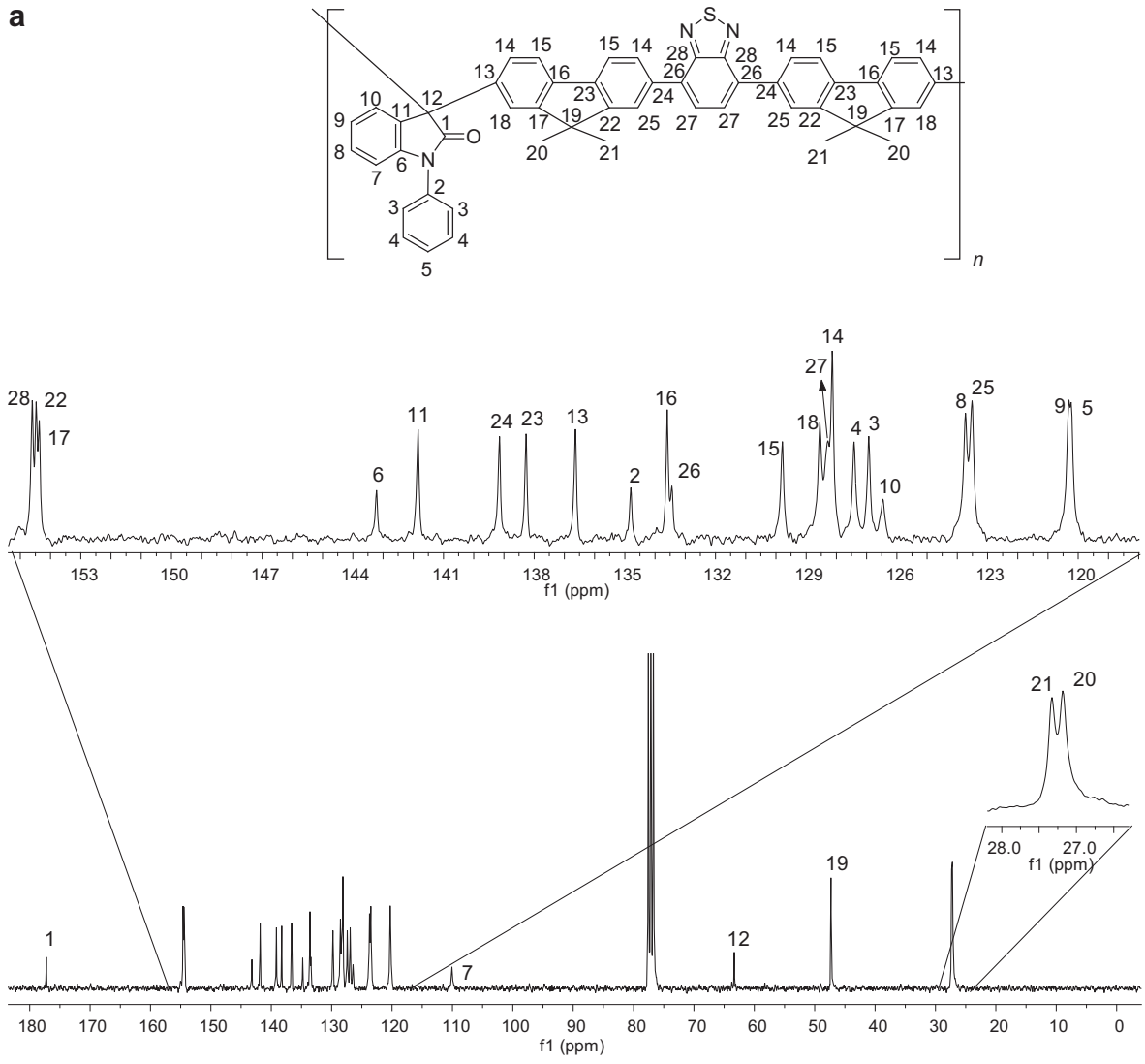

Fig. 2. a. ^{13}C NMR spectrum of polymer **PM1** (solution in $CDCl_3$). b. The ^{1}H and ^{13}C NMR spectra of polymer **PM2** (solutions in $CDCl_3$).

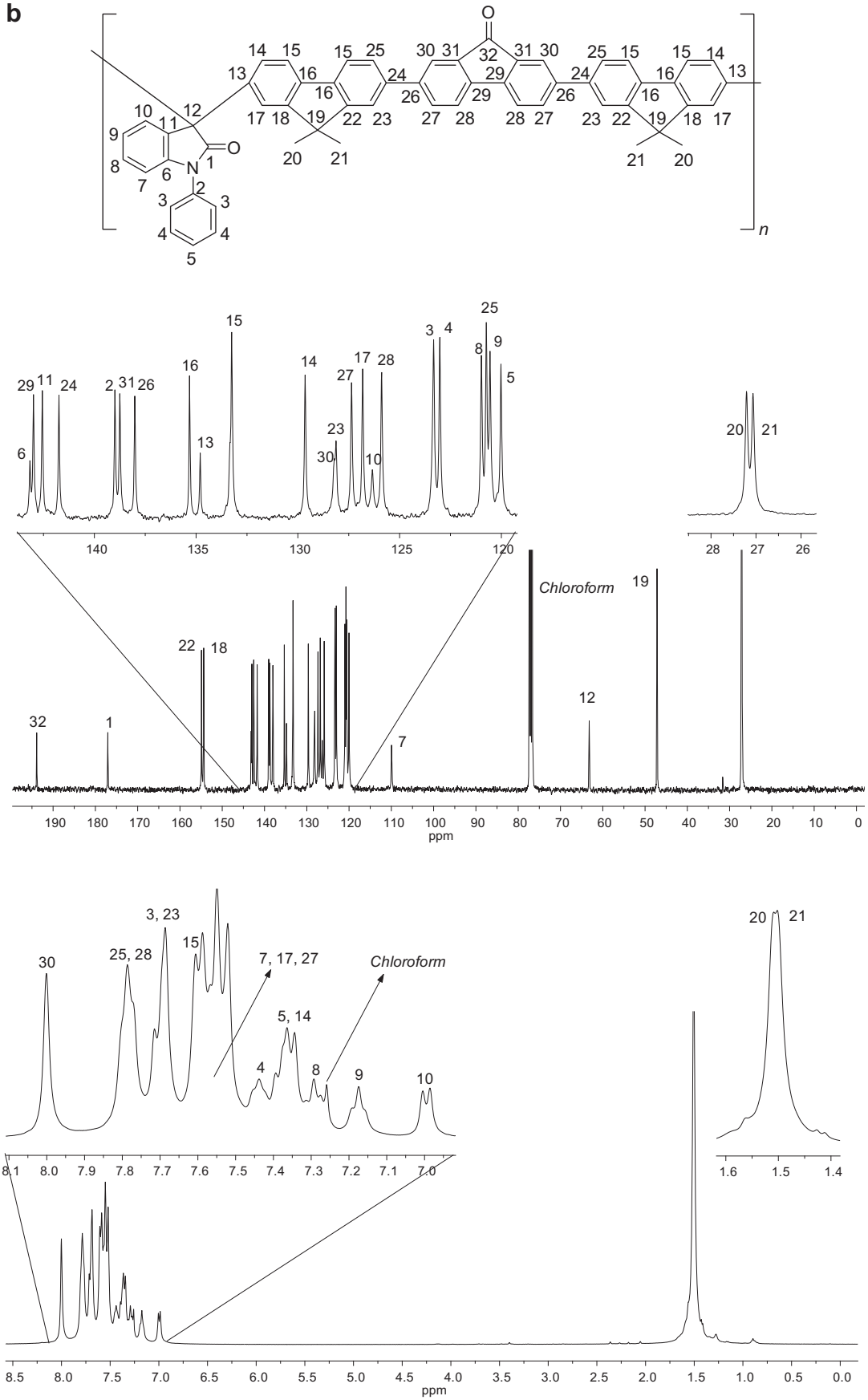

Fig. 2. (*continued*).

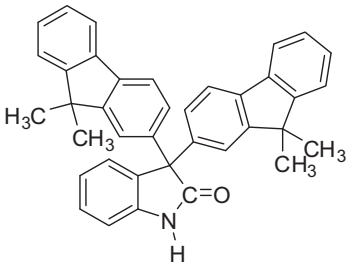

Fig. 3. Chemical structure of the model compound.

[20]. Therefore, these polymers should behave similarly to truly conjugated polymers and show similar properties.

3. Linear and non-lineal optical properties

3.1. Absorption and photoluminescence

Fig. 5 shows the normalized linear absorption and photoluminescence (PL) spectra for all compounds. Absorption bands with main maxima at 316, 348, 324, 354, and 320 nm are found for **M1**, **M2**, **PM1**, **PM2**, and **CPM**, respectively, that are attributed to $\pi-\pi^*$ transition of the conjugated main chain. **M2** also shows a strong peak at 309 nm. **M1**, **PM1** and **CPM** show absorption bands of moderate intensity at 415, 419 and 422 nm, respectively, which are assigned to the $n-\pi^*$ transition of the benzothiadiazole building blocks. **M2** and **PM2** also show a weak low energy band at 454/455 nm that is associated to the $n-\pi^*$ transition of the fluorenone unit [24,25]. These compounds show an intense photoluminescence (PL) and emit light of green and greenish-yellow color (See Fig. 5b). Preliminary results give a quantum yield close to one for some of these compounds, this parameter is being determined by using an integrating sphere and a fluorescence standard with known quantum yield (laser dyes). Currently, two photon absorption (TPA) experiments are conducting. Their PL maxima are located at 538, 573, 538, 578, and 552 nm for **M1**, **M2**, **PM1**, **PM2**, and **CPM** respectively. Table 1 summarizes the absorption and PL maxima.

3.2. Cubic optical non-linearities

The cubic NLO response for these fluorene monomers and polymers was estimated through the use of third-harmonic generation (THG) Maker-Fringes technique [21]. The choice of using this technique to measure $\chi^{(3)}$ is because it allowed us to measure pure electronic NLO effects (important for high bandwidth photonic applications). For these measurements, solid state films were prepared by spin cast. Sample thickness was between 85 and 200 nm. As an example of these experiments, Fig. 6 shows the so called THG Maker-Fringe pattern for a **PM1** film. As reference, the figure also includes the THG pattern measured from the fused silica substrate alone (thickness: 1 mm). These data were obtained at the fundamental near infrared wavelength of 1200 nm (THG signal in 400 nm). From these data is estimated that the third-order non-linear susceptibility of the **PM1** film is of the order of 7.5×10^{-12} esu at such fundamental wavelength. Table 1 summarizes the cubic measurements for these compounds.

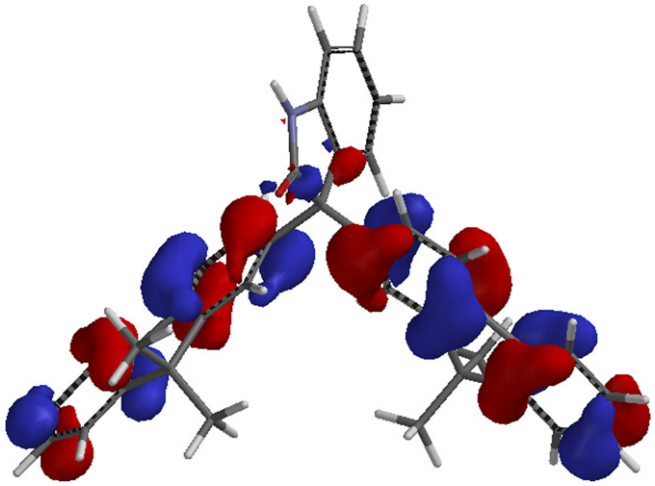

Fig. 4. HOMO of the model compound calculated at HF/3-21G level of theory.

From our measurements, the monomer **M2** and the polymer **PM1** showed the largest cubic susceptibilities $\chi^{(3)}$: 1.0×10^{-11} esu and 7.5×10^{-12} esu, respectively. It seems that $\chi^{(3)}$ value of **M2** fragments depends strongly on conjugation within the unit. Thus, conjugation defects frequently occur in a polymer due to globular conformation of the chain and it may cause a decrease in the cubic non-linearity for **PM2** compared to **M2**. On the other hand, NLO properties of **M1** are mostly related with strongly polarisable central fragment, not with the conjugation along the oligomer. This could be a possible reason in increasing $\chi^{(3)}$ in **PM1** compared with **M1** due to additional contribution of "isatin" unit. It is important to mention that the absorption coefficients (α) at 400 nm for **M1**, **M2**, **PM1**, **PM2** and **CPM** are 1.7, 1.5, 6.5, 1.4 and 3.8×10^4 cm^{-1}, respectively, so there is not a significant difference between them in the $\chi^{(3)}$ values through three-photon resonance (about a factor of

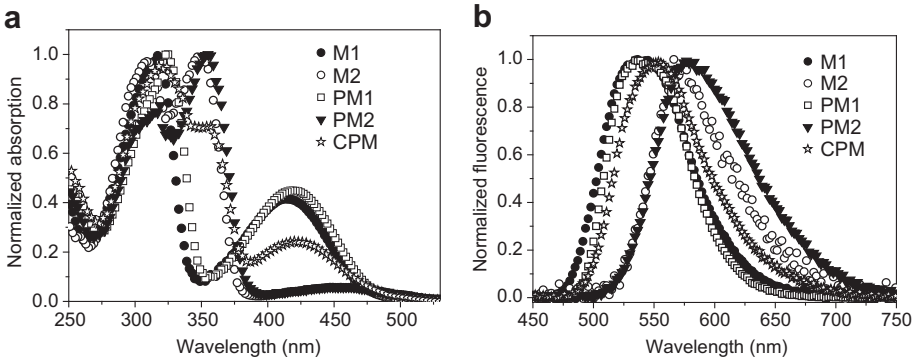

Fig. 5. a. Normalized optical linear absorption of the monomers **M1** and **M2** and the polymers **PM1**, **PM2** and the copolymer **CPM**. b. Normalized photoluminescence of these same compounds. Samples were dissolved in chloroform. A nitrogen laser (337 nm) was used as the pumping light source.

Table 1
Absorbance and fluorescence maxima; absorption coefficient α and $\chi^{(3)}$ values.

Sample	Absorbance[a] λ_{max} (nm)	Fluorescence[a] λ^{PL}_{max} (nm)	$\alpha \times 10^4$ (cm^{-1})[b]	$\chi^{(3)}$ ($\times 10^{-12}$ esu)[c]
M1	316	538	1.7	4.3
M2	348	573	1.5	10.0
PM1	324	538	6.5	7.5
PM2	354	578	1.4	5.9
CPM	320	552	3.8	4.6

[a] In solution (chloroform).
[b] Solid state films: At 400 nm: For THG, fundamental wavelength of 1200 nm.
[c] Solid state films: $\chi^{(3)}$ for fused silica = 3.1×10^{-14} esu at 1200 nm.

<1.5 times for the largest difference on the cubic susceptibility) when using the wavelength of 1200 nm (see Eq. (1) in the Experimental section).

For the well known poly(*p*-phenylenevinylene) (PPV) polymer, $\chi^{(3)}$ is reported to be of the order of 10^{-10}–10^{-11} esu [26], while for poly[2-methoxy-5-(2′-ethyl-hexyloxy)-1,4-phenylenevinylene] (MEH:PPV), a well known conjugated polymer with linear molecular structure, $\chi^{(3)}$ is in the range between 1.5 and 3.5×10^{-11} esu (at 1200 nm) [27]. PPV and MEH:PPV polymers are considered as prototypes of non-linear materials for photonic applications. For some oligomers of PV (PV-*n*), $\chi^{(3)}$ values are reported, measured through THG Maker-Fringe technique, on the order of 10^{-11}–10^{-13} esu [26,28]. So, the $\chi^{(3)}$ values for our synthesized fluorene derivatives, estimated from the THG Maker-Fringe technique, are in the interval of some PV oligomers and slightly smaller that for MEH-PPV. In regards to third-order NLO properties, the standard techniques used to measure non-linearities include Z-scan, DFWM, Kerr effect and Maker-Fringe (THG). It must be observed that these techniques determine different tensor values of $\chi^{(3)}$. In addition to these different characterization techniques, the variety of wavelengths employed, pulse duration of the lasers and the fact that most of non-linear characterization is performed with solutions make that the comparison between the optical non-linearities reported in the literature for similar molecules is not straightforward. For example, the third-order non-linear optical properties of fluorene polymers in $CHCl_3$ were measured using a femtosecond time-resolved optical Kerr effect technique obtaining $\chi^{(3)}$ of the order of 10^{-14}–10^{-15} esu [18]. In PPV films, by using DFWM, $\chi^{(3)}$ of the order of 10^{-10} esu employing fs laser pulses at 1200–1800 nm was estimated [29].

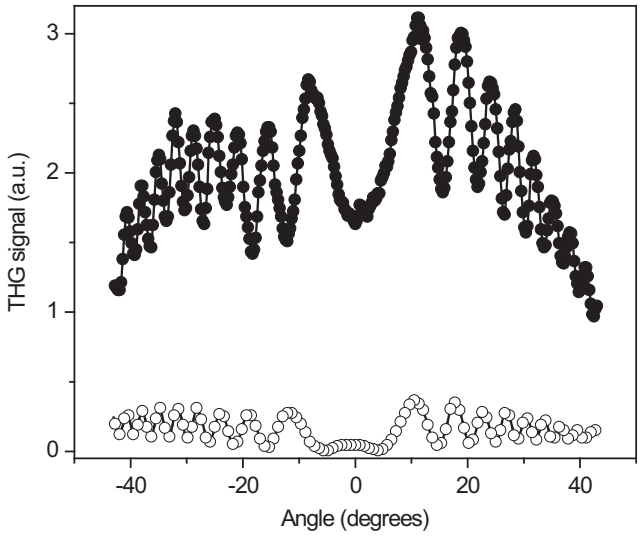

Fig. 6. THG Maker-fringe pattern for a 101 nm-thin polymer film of compound **PM1** (filled circles) and for a 1-mm-thick substrate without a film deposited on it (open circles). The fundamental wavelength was 1200 nm.

The wavelength dependence of the third-order non-linear susceptibility for compound **PM1** was also determined (See Fig. 7a). To make clear the multi-photon resonance, Fig. 6 includes the linear absorption spectrum of the film (top and right axes). Note that the wavelength scales are arranged in such a way that the bottoms scale is 3 times the top one. Thus, according to the absorption peak located at 418 nm (see also Fig. 5), it is observed a slight enhancement (about a factor of 1.5) on cubic non-linearities due to three-photon resonances. For comparison, this figure (Fig. 7b) also includes the dispersion measured under the same experimental conditions on a MEH:PPV film.

3.3. Evaluation of γ

Because in the literature most of molecular characterization is performed using solutions, then the second molecular hyperpolarizability γ is more frequently reported than $\chi^{(3)}$. Static average second hyperpolarizabilities were estimated for **M1** and **M2** theoretically. Molecular geometry was optimized at B3LYP/6-31G(d)

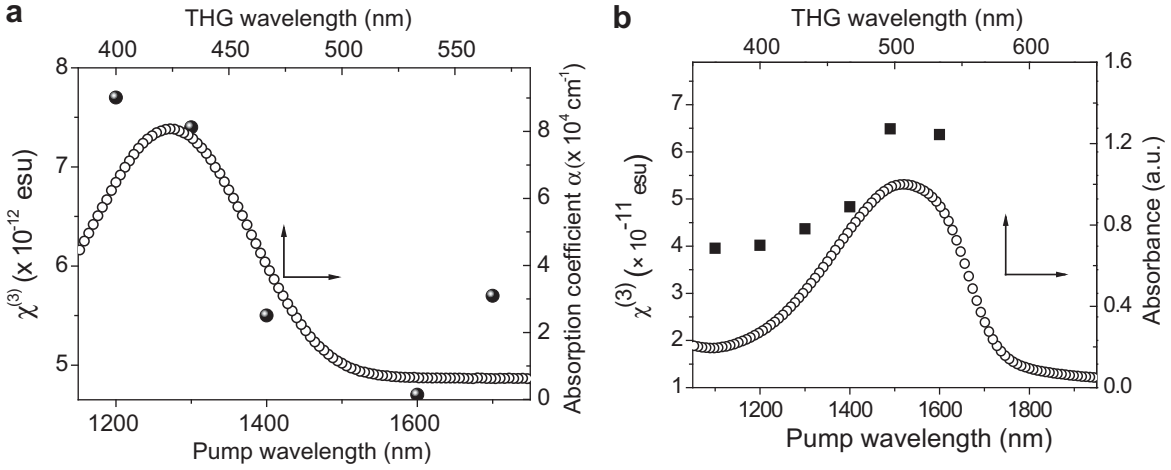

Fig. 7. Wavelength dependence of the third-order non-linear susceptibility (bottom and left axes): a. for the polymer **PM1** film (Filled circles). b. As comparison, for MEH:PPV polymer film (Filled squares) [14]. As reference, the absorption for the films is included (top and right axes) (Open circles).

level of theory in gas phase. Larger 6-311+G(d,p) was applied for the calculation of γ using B3LYP/6-31G(d) optimized geometry. CPHF method as implemented in Jaguar 7.6 suite of programs [23] was used for calculations. The γ calculated for **M1** and **M2** were found to be of 1.03×10^{-33} and 1.26×10^{-33} esu, respectively. It seems that larger conjugated system that exists in **M2** contributes more than highly polarisable S atom of **M1**. This hypothesis is also confirmed by the fact that not only second polarisabilities but calculated linear polarisabilities and first hyperpolarizabilities are larger for **M2**.

The magnitude of γ calculated theoretically was compared with the experimental values. In solid films γ is given by $<\gamma> = \chi^{(3)}/L^4N_s$ where N_s is the number density of molecules in the compound film and $L = (n^2 + 2)/3$ is the correction factor due to local field effects [18,30], n being the refractive index. In our case, the second hyperpolarizabilities are estimated to have values of 0.96×10^{-33}, 2.35×10^{-33}, 311×10^{-33} and 240×10^{-33} esu for **M1** (M_w = 536.23 g/mol), **M2** (M_w = 564.25 g/mol), **PM1** (M_w = 122,000 g/mol) and **PM2** (M_w = 85,500 g/mol), respectively. These estimations were made for a wavelength of 1200 nm. As seen, absolute values for γ (theoretical values) correlate with experimentally measured $\chi^{(3)}$ values. It is noteworthy that **M1**, having S atom shows lower $\chi^{(3)}$ and γ values compared to **M2**.

As we pointed out previously, it is no easy to compare cubic non-linearities due to the different techniques and experimental conditions used for different groups. For instance, for some fluorene polymers in $CHCl_3$ where a femtosecond time-resolved optical Kerr effect technique was used, γ values of 10^{-30}–10^{-31} esu were obtained [18]. In Ref. [31] is reported that the molecular second-order hyperpolarizability for thin films of the thienyleneethynylene oligomers in poly(methyl methacrylate), measured by THG Marker fringe technique, is 2.30×10^{-33} esu. By using Z-scan technique at 800 nm with 100-fs laser pulses, in Ref. [32] an estimated γ value up to 2.5×10^{-32} esu for oligomers of PV was indicated and in Ref [28] a γ of the order of 10^{-32} esu by THG Maker-fringe technique was reported. It is important to point out that effective comparisons must be carried out with compounds tested under the same technique, *i.e.*, measurement of non-linearities with same origin such as γ ($-3\omega,\omega,\omega,\omega$) or γ ($\omega,\omega,-\omega,\omega$). In our case, the use of THG-Maker-fringes technique at infrared wavelength assured that the measurement of $\chi^{(3)}$ ($-3\omega,\omega,\omega,\omega$) has pure electronic origin, while other methods, such as Z-scan ($\chi^{(3)}$ ($\omega,\omega,-\omega,\omega$)), might include several competing contributions (for instance: thermal effects) to the overall non-linear measurements. Nevertheless, it must be also mentioned that although the relatively large values of γ measured through THG technique only looked at electronic effects, the observed partial three-photon resonance (see Fig. 7) could imply time response limitations for high bandwidth photonic applications.

4. Conclusions

Two new fluorene monomers (**M1** and **M2**) and two corresponding polymers (**PM1** and **PM2**) and a copolymer (**CPM**) were synthesized and characterized. Transparent, strong, and flexible films could be cast from polymer solutions. With respect to their NLO properties, it seems that $\chi^{(3)}$ value of **M2** fragments depends strongly on conjugation within the unit. Thus, conjugation defects frequently occur in polymers due to globular conformation of polymer chain decreasing cubic non-linearity for **PM2** compared to that one for **M2**. On the other hand, non-linear optical properties of **M1** are mostly related with strongly polarisable central fragment, not with the conjugation along the oligomer. This could be the reason in increasing $\chi^{(3)}$ in **PM1** in comparison with cubic susceptibility for **M1** with the additional contribution of "isatin" unit. This conclusion can also be supported by the theoretical evaluation of γ, which to some, extent correlates with experimentally determined $\chi^{(3)}$ for oligomers **M2** and **M1**. From our experimental and theoretically results, it can be induced that compounds possessing high $\chi^{(3)}$ values, not due to proper conjugation but due to highly polarisable individual fragments, seem to be the best candidates for incorporation into polymer chain in order to obtain a polymer with good third-order non-linear optical properties.

5. Experimental

Unless otherwise indicated, all starting materials were obtained from commercial suppliers and were used without further purification. ^{1}H and ^{13}C NMR data were obtained on a Bruker ARX 400-spectrometer. Chemical shifts are given in parts per million (ppm) using residual solvent protons as internal standards. Splitting patterns are designated as "s" (singlet), "d" (doublet), "t" (triplet), and "m" (multiplet). Low-resolution mass spectra were obtained on a Varian MAT 311A operating at 70 eV (Electron Impact, EI) and reported as m/z and percent relative intensity. FD masses were obtained on a ZAB 2-SE-FDP. Elemental analyses were performed at the University of Wuppertal, Department of Analytical Chemistry, using a Perkin Elmer 240B. The inherent viscosities of 0.2% polymer solutions in 1-methyl-2-pyrrolidinone (NMP) were measured at 25 °C using an Ubbelohde viscometer. The chromatography system was equipped with three Waters styragel columns at 40 °C with THF as the solvent at a flow rate of 1.0 mL/min. The SEC-MALS measurements were performed at 25 °C using a separation system comprising two size-exclusion columns (a Waters HSPgel HR MB-L and a HR MB-B) with a molecular weight range from 5×10^2 to 7×10^5 and 1×10^3 to 4×10^6, respectively. The light scattering measurements were carried out on a Dawn Eos multi-angle light scattering (MALS) instrument (Wyatt Technology, Santa Barbara, CA).

5.1. Monomer syntheses

5.1.1. 2-Bromo-9,9-dimethylfluorene

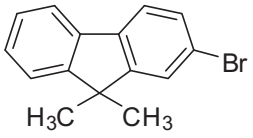

Aqueous sodium hydroxide solution (40 mL, 50%) and iodomethane (31.9 g, 225 mmol) were added to a solution of 2-bromofluorene (25 g, 102 mmol) and tetrabutylammonium bromide (9.9 g, 31 mmol) in 75 mL of DMSO at 45 °C. The mixture was stirred at 45 °C for 2 h and then poured into water (100 mL). The mixture was extracted two times with diethylether. The combined organic phases were washed with brine, water and dried over Na_2SO_4. After evaporation of the solvent the residue was purified by column chromatography with hexane as eluent to receive a colorless oil, that solidified under stirring in vacuum to yield 27.8 g (80%) of 2-bromo-9,9-dimethylfluorene.

^{1}H NMR (400 MHz, $CDCl_3$): δ: ppm. 7.3–7.7 (m, 6H, Ar-H), 1.49 (s, 6H, CH3) ppm.

^{13}C NMR (100 MHz, $CDCl_3$): δ = 155.7, 153.3, 138.2, 130.1, 127.7, 127.2, 126.1, 122.6, 121.4, 121.0120.0, 47.1, 27.0 ppm.

LR-MS (EI, m/z): 178 (100.0), 272 [M^+] (93), 274 (93), 273 (45), 274 (43).

5.1.2. 9,9-Dimethyl-2-(4,4′,5,5′-tetramethyl-1,3,2-dioxaborolano) fluorene

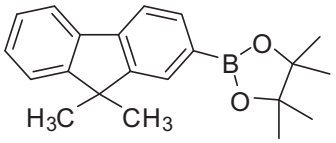

A flame dried 500 mL flask was charged with 2-bromo-9,9-dimethylfluorene (15 g, 55 mmol) and sealed under argon. Dry hexane (250 mL) and THF (50 mL) were added and the mixture cooled to −78 °C. n-BuLi (55 mmol) was added, the mixture stirred for 10 min and allowed to warm up to 0 °C. The solution was cooled again to −78 °C, and 2-isopropoxy-4,4′,5,5′-tetramethyl-1,3,2-dioxaborolane (71 mmol) added at once. The reaction mixture was stirred at room temperature for 12 h. The mixture was poured into water and extracted with chloroform. The solution was evaporated to dryness and the residue purified by column chromatography using hexane/ethyl acetate (95:5) as eluent. After removing the solvent the remaining solid was recrystallized from hexane to afford 12.5 g of 9,9-dimethyl-2-(4,4′,5,5′-tetramethyl-1,3,2-dioxaborolano)fluorene as a white solid in 71% yield.

^{1}H NMR (400 MHz, $CDCl_3$): δ = 7.73–7.90 (m, 4H), 7.32–7.47 (m, 3H), 1.52 (s, 6H), 1.39 (s, 12H) ppm.

^{13}C NMR (100 MHz, $CDCl_3$): δ = 154.3, 152.8, 142.2, 139.0, 133.9, 127.8, 127.7, 126.9, 122.6, 120.4, 119.3, 83.7, 46.8, 27.1, 24.9 ppm.

LR-MS (EI, *m*/*z*): 319.9 [M^+] (100.0), 304.6 (90.0).

2,7-Dibromofluorene, 2,7-dibromofluorene-9-one, and 4,7-dibromobenzo[1,2,5]thiadiazole are known compounds:

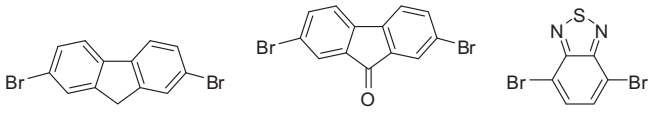

General procedure for the Suzuki-type coupling: 9,9-Dimethyl-2-(4,4′,5,5′-tetramethyl-1,3-2-dioxaborolano)fluorene (10.4 mmol), the corresponding dibromo compound (3.25 mmol), sodium carbonate (130 mmol) and aliquat 336 (1.3 mmol) were dissolved in a mixture of 90 mL of toluene and 60 mL of water under argon. The $Pd(PPh_3)_4$ catalyst (0.162 mmol) was subsequently added and the reaction mixture was stirred for 48 h at 100 °C. After cooling down to room temperature the mixture was extracted with dichloromethane and washed with aqueous 2 N HCl solution, concentrated $NaHCO_3$-solution and brine. The organic phase was dried over Na_2SO_4 and the solvent removed under vacuum. The solid precipitate was recrystallized from heptane/dichlormethane (1:1) to obtain the trimeric products in 78–82% yield.

*5.1.3. 4,7-Bis[2′-(9′,9′-dimethyl)fluorenyl]benzo[1,2,5]thiadiazole (**M1**)*

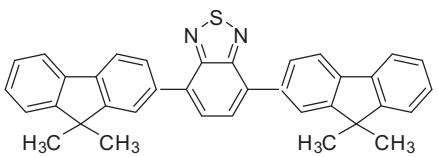

^{1}H NMR (600 MHz, $C_2D_2Cl_4$): δ = 8.03 (dd, 4H), 7.88 (dd, 4H), 7.79 (dd, 2H), 7.48 (dd, 2H), 7.36 (m, 4H), 1.57 (s, 12H) ppm.

^{13}C NMR (150 MHz, $C_2D_2Cl_4$): δ = 154.5, 154.4, 154.3, 139.7, 139.0, 136.7, 133.6, 128.8, 128.4, 127.9, 127.4, 123.9, 123.0, 120.6, 120.4, 47.3, 27.6 ppm.

*5.1.4. 2,7-Bis[2′-(9′,9′-dimethyl)fluorenyl]fluorene-9-one (**M2**)*

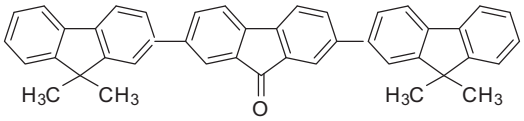

^{1}H NMR (600 MHz, $C_2D_2Cl_4$): δ = 7.98 (d, 2H), 7.81 (dd, 2H), 7.77 (d, 2H), 7.73 (dd, 2H), 7.68 (d, 2H), 7.62 (d, 2H), 7.60 (dd, 2H), 7.45 (dd, 2H), 7.34 (m, 4H), 1.54 (s, 12H) ppm.

^{13}C NMR (150 MHz, $C_2D_2Cl_4$): δ = 194.0, 154.5, 154.0, 143.0, 139.2, 138.7, 138.6, 135.2, 133.5, 127.7, 127.2, 125.9, 123.0, 122.8, 121.0, 121.0, 120.5, 120.3, 47.0, 27.3 ppm

5.1.5. Synthesis of polymers

*Synthesis of polymer **PM1***: 4,7-Bis[2′-(9′,9′-dimethyl)fluorenyl] benzo[1,2,5]thiadiazole (**M1**) (0.416 g, 0.80 mmol) and *N*-phenylisatin (0.179 g, 0.80 mmol) were dissolved in dichloromethane (2.3 mL) and then trifluoromethanesulfonic acid (0.7 mL) was added and the mixture was stirred at room temperature for 5 h. The resulting green, viscous solution was then poured slowly into methanol (200 mL). The precipitated, yellow fibres were filtered off, extracted with refluxing methanol and acetone, and dried at 100 °C under vacuum. The resulting pure yellow polymer **PM1** (0.562 g, 98.2% yield) had an inherent viscosity η_{inh} = 0.90 dL/g (NMP).

The polymer **PM2** was obtained by the following procedure. 2,7-Bis[2′-(9′,9′-dimethyl)fluorenyl]fluorene-9-one (**M2**) (0.240 g, 0.42 mmol), *N*-phenylisatin (0.095 g, 0.42 mmol), dichloromethane (1.3 mL) and trifluoromethanesulfonic acid (0.3 mL) were stirred at room temperature for 24 h. The resulting transparent red viscous solution was poured into methanol, and orange fibres were filtered off, extracted with refluxing methanol and acetone, and dried at 80 °C in an oven. The resulting polymer **PM2** (0.326 g, 99.7% yield) had an inherent viscosity η_{inh} = 0.51 dL/g (NMP).

Copolymer **CPM** was obtained by analogous procedure. 4,7-Bis[2′-(9′,9′-dimethyl)fluorenyl]benzo[1,2,5]thiadiazole (**M1**) (0.208 g, 0.40 mmol), 2,7-Bis[2′-(9′,9′-dimethyl)fluorenyl]fluorene-9-one (**M2**) (0.226 g, 0.40 mmol), *N*-phenylisatin (0.179 g, 0.80 mmol), dichloromethane (2.3 mL) and trifluoromethanesulfonic acid (0.7 mL) were stirred at room temperature for 4.5 h. The resulting transparent brown viscous solution was poured into methanol, and yellowish fibres were filtered off, extracted with refluxing methanol and acetone, and dried at 80 °C in an oven. The resulting polymer **CPM** (0.59 g, 49.4% yield) had an inherent viscosity η_{inh} = 0.85 dL/g (NMP).

The structure of the polymers synthesized was confirmed by ^{1}H and ^{13}C NMR analysis.

5.1.6. Optical measurements

Cubic non-linearities were studied in solid state (solid films), **M1**, **M2**, **PM1**, **PM2** and **CPM** were dissolved in chloroform. Films were deposited on fused silica substrates (1 mm-thick) by using the spin coating technique. The prepared films had thickness between 85 and 200 nm with good optical quality showing negligible light scattering at visible and NIR wavelengths. Absorption spectra of spin-coated films were obtained with a spectrophotometer (Perkin–Elmer Lambda 900). Sample thickness was measured by using a Dektak 6M profiler.

THG Maker-fringes setup is reported elsewhere [33,34]. Briefly, it consisted of a Nd-YAG laser-pumped optical parametric oscillator (OPO) that delivered pulses of 8 ns at a repetition rate of 10 Hz. The output of the OPO system was focused into the films with a 30-cm focal-length lens to form a spot with a radius of approximately 150 μm. Typical energies in our measurements were set at 1 mJ per

pulse at sample position (corresponding to peak intensities of ~0.18 GW/cm^2). The third-harmonic beam, as a bulk effect, emerging from the films was separated from the pump beam by using a color filter and detected with a PMT and a Lock-in amplifier. The THG measurements were performed for incident angles in the range from −40° to 40° with steps of 0.27°. All the experiment was computer controlled.

In the Maker-fringes technique, the third-harmonic peak intensity $I^{3\omega}$ from the substrate-film structure is compared to one produced from the substrate alone. Then, the non-linear susceptibility $\chi^{(3)}$ in a film of thickness L_f is determined from [35]:

$$\chi^{(3)} = \chi_s^{(3)} \frac{2}{\pi} L_{c,s} \left(\frac{\alpha/2}{1 - \exp\left(\alpha L_f/2\right)} \right) \left(\frac{I_f^{3\omega}}{I_s^{3\omega}} \right)^{1/2} \quad (1)$$

where $\chi_s^{(3)}$ and $L_{c,s}$ are the non-linear susceptibility and coherence length, respectively, for the substrate at the fundamental wavelength, and α is the film absorption coefficient at the harmonic wavelength. In our calculation we considered $\chi_s^{(3)} = 3.1 \times 10^{-14}$ esu for the fused silica substrate and $L_{c,s}$ (9 μm at 1200 nm) was calculated from tabulated values of the refractive index [33,34]. Our samples satisfied the condition $L_f \ll L_{c,s}$ in which the Eq. (1) is valid.

Acknowledgments

Authors acknowledge the financial support from CONACYT Mexico (grants 60942 and 55250), and support from DGAPA-UNAM (PAPIIT IN 111908). Thanks are due to Dr. G. Cedillo for recording the NMR spectra, S. L. Morales and E. Fregoso-Israel for assistance with thermal and spectroscopic analysis, and M. Olmos for film preparation and optical linear characterization.

References

[1] Shirota Y, Kageyama H. Chem Rev 2007;107:953–1010.
[2] Saragi TPI, Spehr T, Siebert A, Fuhrmann-Lieker T, Salbeck J. Chem Rev 2007;107:1011–65.
[3] Park JW, Park SJ, Kim YH, Shin DC, You H, Kwon SK. Polymer 2009;50:102–6.
[4] Jung IH, Jung YK, Lee J, Park JH, Woo HY, Lee JI, et al. J Polym Sci A Polym Chem 2008;46:7148–61.
[5] Ono K, Saito K. Heterocycles 2008;75:2381–413.
[6] Chen H, Cai XR, Xu ZG, Zhang T, Song BF, Li Y, et al. Polym Bull 2008;60:581–90.
[7] Peng ZK, Tao SL, Zhang XH, Tang JX, Lee CS, Lee ST. J Phys Chem C 2008;112:2165–9.
[8] Tang WH, Ke L, Tan LW, Lin TT, Kietzke T, Chen ZK. Macromolecules 2007;40:6164–71.
[9] Kong QG, Zhu D, Quan YW, Chen QM, Ding JF, Lu JP, et al. Chem Mater 2007;19:3309–18.
[10] Jaramillo-Isaza F, Turner ML. J Chem Mater 2006;16:83–9.
[11] Guang SH, Loon-Seng T, Qingdong Z, Paras N. Chem Rev 2008;108:1245–330.
[12] Hwan MK, Bong RC. Chem Commun 2009:153–64.
[13] Terenziani F, Katan C, Badaeva E, Tretiak S, Blanchard-Desce M. Adv Mater 2008;20:4641–78.
[14] Castro-Beltran R, Ramos-Ortiz G, Jim CKW, Maldonado JL, Häußer M, Peralta D, et al. Appl Phys B-Lasers 2009;97:489–96.
[15] Mongin O, Porres L, Charlot M, Katan C, Blanchard-Desce M. Chem Eur J 2007;13:1481–98.
[16] Belfield KD, Morales AR, Kang BS, Hales JM, Hagan DJ, Van Stryland EW, et al. Chem Mater 2004;16:4634–41.
[17] Thomas III SW, Joly GD, Swager TM. Chem Rev 2007;107:1339–86.
[18] Zhan XW, Liu YQ, Zhu DB, Huang WT, Gong QH. Chem Mater 2001;13:1540–4.
[19] Sanguinet L, Williams JC, Yang ZY, Twieg RJ, Mao GL, Singer KD, et al. Chem Mater 2006;18:4259–69.
[20] Smith M, March J. March's advanced organic chemsitry. 6th ed. Willey & Sons; 2007. p. 45.
[21] Kajzar F, Messier J, Rosilio CJ. Appl Phys 1986;60:3040–4.
[22] Hernández MCG, Zolotukhin MG, Maldonado JL, Rehmann N, Meerholz K, King S, et al. Macromolecules 2009;42:9225–30.
[23] Jaguar, version 7.5, Schrodinger. New York: LLC; 2008.
[24] Zojer E, Pogantsch A, Hennebicq E, Beljonne D, Brédas JL, Scandiucci de Freitas P, et al. J Chem Phys 2002;117:6794–802.
[25] Kulkarni AP, Kong X, Jenekhe SA. J Phys Chem B 2004;108:8689–701.
[26] Mathy A, Ueberhofen K, Schenk R, Gregorius H, Garay R, Müllen K, et al. Phys Rev B 1996;53:4367–76.
[27] Bahtiar A, Koynov K, Ahn T, Bubeck C. J Phys Chem B 2008;112:3605–10.
[28] Koynov K, Bahtiar A, Bubeck C, Muhling B, Meier HJ. Phys Chem B 2005;109:10184–8.
[29] Samoc M, Samoc A, Luther-Davies B. Opt Express 2003;11:1787–92.
[30] Whittall IR, McDonagh AM, Humphrey MG, Samoc M. Adv Organomet Chem 1999;43:349–405.
[31] Geisler T, Petersen JC, Bjørnholm T, Fischer E, Larsen J, Dehu C, et al. J Phys Chem 1994;98:10102–11.
[32] Wong MS, Li ZH, Shek MF, Samoc M, Samoc A, Luther-Davies B. Chem Mater 2002;14:2999–3004.
[33] Ramos-Ortiz G, Maldonado JL, Meneses-Nava MA, Barbosa-García O, Olmos-López M, Cha M. Opt Mater 2007;29:636–41.
[34] Victorovna-Lijanova I, Reyes-Valderrama MI, Maldonado JL, Ramos-Ortiz G, Tatiana K, Martínez-García M. Tetrahedron 2008;64:4460–7.
[35] Wang XH, West DP, McKeown NB, King TA. J Opt Soc Am B 1998;15:1895–903.